Discrimination of Disposable Vapes from Batteries Using the Magnetic Polarizability Tensor

DOI:
10.1109/JSEN.2024.3381716

Document Version
Accepted author manuscript

Discrimination of Disposable Vapes from Batteries Using the Magnetic Polarizability Tensor

Kane C. Williams, *Graduate Member, IEEE*, John L. Davidson, Michael D. O'Toole, *Member, IEEE*, Anthony J. Peyton

***Abstract*— Disposable vapes pose an environmental and fire hazard to waste streams when disposed of incorrectly. The lithium battery inside disposable vapes can produce an exothermic reaction when the lithium inside the battery is inadvertently exposed to air and moisture. New sensing technologies may be needed to screen waste streams for these vape hazards and this paper considers the potential of inductive techniques based on the magnetic polarisability tensor (MPT) representation. The MPT can be described by three complex components based on a target regardless of orientation. In this paper, the rank 2 MPT is measured and calculated for 10 vapes and 37 batteries for 28 logarithmically spaced frequencies from 119 Hz to 95.4 KHz. The 168 features of each object are reduced down to 2 features using principal component analysis (PCA) and linear discriminant analysis. The reduction of the features allows for the visualisation and grouping of the objects. Three clear groups of objects can be seen when the maximum feature scales the measurement and a two-component PCA transform is applied. The first group is the vapes, which are grouped away from the other batteries. The second is the batteries, which are grouped by size. Finally, zinc batteries are grouped away from the rest due to their case material.**

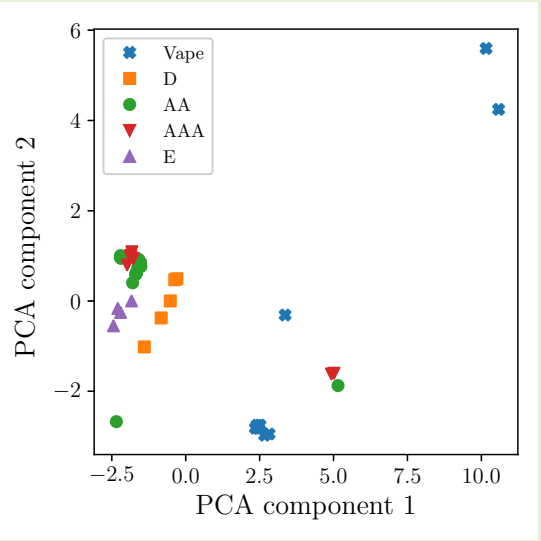

***Index Terms*— electromagnetic induction, magnetic polarizability tensor (MPT), disposable vapes, recycling, waste recovery.**

I. Introduction

The use of disposable or 'single-use' vapes is a worldwide environmental concern. In the US, the sales of e-cigarettes increased from 15.5 million in January 2020 to 22.7 million units per 4-week period in December 2022 [1]. In the UK, it is estimated that approximately 14 million single-use vapes are sold each month, with over 50% disposed of incorrectly [2], [3]. Disposable vapes are non-rechargeable devices that typically contain a pre-filled 2 ml of e-cigarette liquid and allow for approximately 600 user inhalations. They are advertised as cheap and disposable once used. Disposable vapes tend to have an outer plastic casing to protect the internal contents. The vape usually consists of a lithium battery, used to power the device, which connects to a small printed circuit board containing a control chip, which connects to a thin copper heating element placed inside a sponge soaked in the vape liquid. When the user applies pressure to the mouthpiece, the control chip turns on an LED indicator and connects the battery to the copper heating element. The heating element heats the soaked sponge, creating an aerosol inhaled by the user. When the battery charge is low, the LED flashes, indicating a low battery, leading to the disposal of the vape.

Vapes contain non-degradable plastics, copper and lithium-ion batteries. The UK classifies vapes as waste electrical and electronic equipment (WEEE) and, as such, should be disposed of appropriately in accordance with local WEEE recycling regulations [2], [4]. Under WEEE regulations, a producer of electrical products must finance the collection and treatment of their products when they become waste [2]. However, many single-use vape users are either unaware that these products are recyclable or choose to discard the devices inappropriately. Consequently, many disposable vapes are discarded in public bins or become part of the general litter in public spaces [2]. A report by Material Focus found 73% of UK vapers say they

 This work was supported by the UK Engineering and Physical Sciences Research Council (P122584)

The authors are with the Department of Electrical and Electronic Engineering, The University of Manchester, Manchester M13 9PL, U.K. (e-mail: kane.williams@manchester.ac.uk; j.davidson-2@manchester.ac.uk; michael.otoole@manchester.ac.uk; a.peyton@manchester.ac.uk).

throw away single-use vapes, with 33% of 16-18 year-olds throwing away their vapes in the bin at school or work [5].

The lithium used for the vape batteries thrown away in the UK alone totals 10 tonnes of lithium per year [2]. Lithium is an essential resource, reflected by declarations such as the UK government assigning lithium as highly critical [6], [7]. In 2006, the EU set out the European Battery Directive 2006/66/EC with a target of 45% for collection by September 2016. Collection schemes were set up to allow used batteries to be returned to the location they were bought. In 2023, the EU adopted the new battery regulation 2023/1542, which regulates the batteries throughout their life cycles. The regulation set a target of 63% by 2027 and 73% by 2030 for producers to collect waste batteries. Another key target was that 50% of lithium in waste batteries must be recovered by 2027, increasing to 80% by the end of 2031. Further requirements were set, focused on electric vehicle batteries, with the mandatory minimum recovery of different elements, including lithium.

Recent assessments suggest the production scale of lithium must be increased to match the demand over the next few decades [8], as previously it was reported that the lithium demand would be greater than the lithium supply available without effective recycling [9]. The reported deficit between 2020 and 2050 between the supply and demand of lithium can only be sustained with suitable recycling methods [8].

The lithium batteries also pose a fire risk when disposed of incorrectly. When a lithium battery is not correctly discharged, the lithium within the battery can react to the air and moisture when crushed or shredded, leading to an exothermic reaction [10], [11]. Lithium batteries placed into the mainstream waste can pass through a shredder, which can tear open the battery, causing a fire by igniting other waste present. It has been reported that lithium batteries cause around 48% of waste fires in the UK each year, with a cost of £158 M/p.a. [12], [13]. Sweden has, on average, more than one fire per week at waste facilities [14]. A notable fire in a Norwegian WEEE stream in 2014 took 36 hours to extinguish, where the extinguishing water was discharged into the nearby stream, causing contamination [14], [15].

Research has been published on techniques to detect and remove batteries in a waste stream and focused on general batteries, not those inside vapes. The techniques currently researched for the detection and removal of batteries are magnetic induction, sieves, magnets, vision systems, x-ray and electrodynamics [10], [16]

Novel and robust methods of detecting disposable vapes from other waste materials are of vital and timely importance. This study explores using magnetic induction to determine the magnetic polarizability tensor (MPT) of vapes and different batteries. As the dominant metal content in a vape is its battery, other batteries of similar sizes, which would potentially be present in a waste stream, were used to assess the efficacy. Batteries should not be sent to landfills due to the potential of soil and groundwater contamination; however, many still do [17], [18]. An induction system does not need a line of sight to the target, which, in this work, would be the battery located inside a vape. We measure 28 frequencies to allow for more information on the object for better discrimination, followed by dimension reduction techniques to allow visualisation and reduction of features of the measurements.

Electromagnetic induction has been used in previous work for the discrimination of scrap metal within waste streams [19]–[21] with other work using magnetic induction spectroscopy (MIS) [22]–[26]. MIS has also been used to differentiate batteries based on size and shape [16]. The MPT has been researched for the detection and classification of metal objects for different scenarios. The scenarios include unexploded ordnance detection [27]–[30], anti-personal landmine detection [31]–[36] and walk through metal detectors [37]–[41].

The contribution of this article is twofold: First, we demonstrate the detection of vapes and batteries within an electromagnetic field using a coil system and the ability to calculate the MPT. Second, we show how the many features of the MPT can be reduced to 2 using dimension-reduction techniques. The reduction of data allows for visualisation and discrimination between batteries and vapes.

II. Theory

A. Magnetic polarizability tensor (MPT)

An object's features affect its MPT, which includes the shape, size, orientation, conductivity and permeability of the component parts [42], [43]. The MPT also depends on the electromagnetic frequency the object is exposed to. The mathematical descriptions of the MPT can be found in other literature which gives a full mathematical description which underpin the engineering approximations [44]–[47]. Ledger et al. [48] have shown a mathematical proof of the generalized MPT, which justifies using a rank 2 MPT when the object is present in a uniform field. For clarity and conciseness, only the equations needed to calculate the Rank 2 MPT are reported in this section.

$$\mathbf{M}(f) = \begin{bmatrix} M'_{xx} + jM''_{xx} & M'_{xy} + jM''_{xy} & M'_{xz} + jM''_{xz} \\ M'_{xz} + jM''_{xy} & M'_{yy} + jM''_{yy} & M'_{yz} + jM''_{yz} \\ M'_{xz} + jM''_{xz} & M'_{yz} + jM''_{yz} & M'_{zz} + jM''_{zz} \end{bmatrix} \tag{1}$$

The MPT is represented as a 3 x 3 matrix of tensor components, which are complex numbers, as shown in (1), which is symmetric and has 6 unique complex components. The excitation frequency is f, which must be low enough for the eddy current approximation to be valid and makes the MPT frequency dependent. The object's orientation affects the eddy current circulating in the object, resulting in a different MPT. At least six unique measurements of an object are needed to construct an MPT, but in practice, more measurements will result in an MPT with less noise and increased accuracy [31].

$$V_{ind} \cong -j2\pi f \mu_0 \boldsymbol{H_{tx}^T} \mathbf{M} \boldsymbol{H_{rx}} \tag{2}$$

The induced voltage V_{ind} on the receive coil is shown in (2). j is the imaginary unit , f is the excitation frequency and μ_0 is the permeability of free space. $\boldsymbol{H_{tx}^T}$ is the transpose of the transmit field in 3D space at the position of the object and $\boldsymbol{H_{rx}}$ is the adjoint magnetic field per unit amp from the receive coil. When V_{ind} is measured and subsequently $\boldsymbol{H_{tx}}$ and $\boldsymbol{H_{rx}}$

are calculated for a defined number of unique orientations a set of linear equations can be created. The linear equations allow an eigenvalue matrix that is orientation-independent for the rank 2 MPT approximation to be created, which is given by the following:

$$\mathbf{M} = \mathbf{R}\mathbf{\Lambda}\mathbf{R}^{\mathbf{T}} \tag{3}$$

Where $\mathbf{R}$ is a rotation matrix based on Euler's theorem. $\mathbf{\Lambda}$ is the diagonal matrix show in (4), which is frequency dependent. As the matrix is frequency-dependent, a wide frequency spectrum would provide more details on an object, which could lead to better discrimination between objects.

$$\mathbf{\Lambda}(f) = \begin{bmatrix} \Lambda'_{xx} + j\Lambda''_{xx} & 0 & 0 \\ 0 & \Lambda'_{yy} + j\Lambda''_{yy} & 0 \\ 0 & 0 & \Lambda'_{zz} + j\Lambda''_{zz} \end{bmatrix} \tag{4}$$

B. Dimension reduction

A common approach in machine learning is to reduce the dimensionality of data to improve accuracy. The reduction of dimensions can allow for easier visualisation and reduction of input features in a machine learning algorithm, which reduces the complexity of a model. Two dimension reduction techniques were used for the following work to reduce measurement dimensions from 168 to 2. The 168 features consist of the real and imaginary components of the three eigenvalues across 28 frequencies.

Principle component analysis (PCA) is a method which identifies the closest axis to the data, then projects the data onto it [49], [50]. The axis chosen should preserve the largest variance of the original data, or the axis which minimises the mean squared distance between the point's new projection and their original positions [49], [51]. PCA is unsupervised and does not use the label of the data. PCA first finds the axis which accounts for the highest variance, followed by the second axis, which is orthogonal to the first, repeated for the number of dimensions of a dataset [49]. The variance ratio of each component can be returned and shows the proportion of the variance of the dataset projected on the given axis, where the total of the variance will add up to 1 [49].

Linear discriminant analysis (LDA) is a method which reduces the number of dimensions of a given input or as a classification algorithm. LDA will find the most discriminate axes between classes, allowing a hyperplane to be defined to project the data, which maximises the separability between the known classes [49]. LDA is a supervised method and needs the label of the data to ensure separability.

III. Method

A. MPT measurement system

The MPT system was first described by Özdeğer et al. [52]. The coil arrangement consists of a transmit coil with a 240 mm diameter, which is wound as nine separate sections (turns: 11:3:5:5:5:5:5:3:11). There are two receive coils with a 220 mm diameter connected in series and wound in opposite directions to produce a gradiometer arrangement, with each receives coil separated into four separate sections (turns: 27:18:18:49:49:18:18:27). The MPT system comprises of bespoke electronics for generation of drive signals, measurement amplification and data acquisition of the coil arrangement.

The target object is placed inside a truncated icosahedron, which allows for 16 unique orientations for the calculation of the MPT [32]. The coil system sweeps 28 logarithmically spaced frequencies from 119 Hz to 95.4 KHz. The coil system and the truncated icosahedron are shown in Fig. 1.

To take a measurement, a reference is needed, which is obtained by a background measurement, followed by a measurement of a target of a known tensor, and then another background measurement. When an object is measured, first, a measurement of the background is taken, followed by four measurements of the object in different orientations, then another background measurement; this is repeated until 16 unique orientations are measured, finishing with a background measurement.

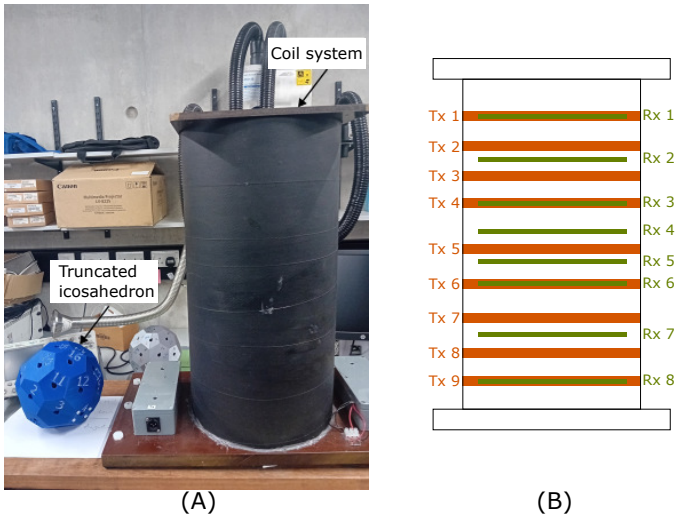

Fig. 1. The MPT measurement system and the truncated icosahedron (A) and coil arrangement showing transmit (Tx) and receive (Rx) coil subsections (B).

B. Dataset

The dataset consists of 10 used disposable vapes and 37 batteries collected from battery recycling points. The vapes include four brands and five different sizes, which are shown in Fig. 2. The batteries used in this study consist of D, AA, AAA and E-block sizes, with their type being a mix of alkaline, Nickel metal hydride (NiMH), lithium, zinc and zinc chloride. Table I shows the sizes and types of batteries used.

C. Software

Sklearn V1.2.2 was used to train PCA and LDA models using the functions "PCA" and "LinearDiscriminantAnalysis". The PCA function returned the variance ratio of each component using ".explained_variance_ratio_". The returned ratio is a number between 0 and 1; for the results, the variance has been converted into a percentage, with 100% representing 1. The LDA model needs to be trained and then

TABLE I
THE SIZE AND TYPES OF BATTERIES MEASURED IN THIS STUDY.

	Size			
Battery Type	D	AA	AAA	E
Alkaline	2	7	4	3
NiMH	3	3	1	0
Lithium	0	5	0	0
Zinc	0	2	2	0
Zinc Chloride	0	4	0	1
Total	5	21	7	4

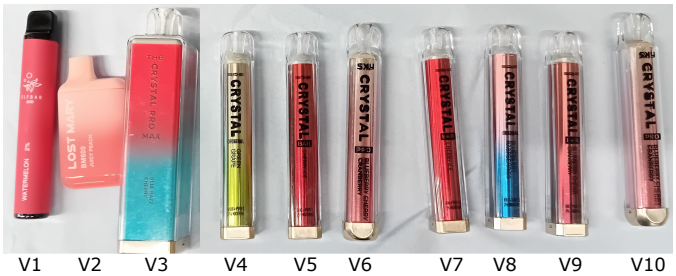

Fig. 2. The ten vapes which were measured in this study.

tested on unseen data. To achieve this, the Sklearn function "LeaveOneOut" was used, which trained an LDA model with all the measurements apart from one. The one measurement not used would be used as the test for the model, which would transform this measurement and subsequently plotted. The process would repeat until every measurement has been used as a test measurement, which allows a result that represents how the algorithm would perform unseen data.

D. Scaling

Two types of scaling were applied. The first was global scaling, where all measurements were used to scale all eigenvalue measurements of each sample between 0 and 1. The second was individual scaling, where each sample measurement was used to scale all eigenvalue measurements of the sample between 0 and 1, independent of the other samples.

IV. RESULT AND DISCUSSION

In the first part of this section, we explore the different eigenvalues of a vape and three batteries using the method described in Section III-A. In the second part, we use PCA and LDA to reduce the 168 dimensions into two dimensions to group and differentiate the vapes from the batteries.

Fig. 3 shows the three eigenvalues of a vape, a NiMH D, alkaline AAA and a lithium AA battery. Fig. 3 shows similar responses for eigenvalues 2 and 3 for all four batteries, which is expected due to the symmetrical nature of a cylinder [53]. The D battery, which is the largest, gives the largest response for all four objects for the real eigenvalues. The D battery gives the largest response for the imaginary eigenvalue 1. However, the vape gives the strongest response for the imaginary eigenvalues 2 and 3. The vape in Fig. 3 shows a difference to the batteries. The vape real response of all three eigenvalues reaches a lower negative value, and the peak of the imaginary component of the eigenvalue is lower in frequency than the batteries in eigenvalues 2 and 3. In eigenvalue 1, the peak of the imaginary component is similar to the D battery but lower in frequency than the other two batteries.

Fig. 4 (a) shows the reduction of the 168 dimension data, which is real and imaginary components of the three eigenvalues across 28 frequencies, to two dimensions using PCA when global scaling is applied. We can see a grouping of D and E-type batteries, though there is one D battery near the cluster of E batteries. AA and AAA batteries are also grouped together, though four batteries are not part of this group. These four batteries are Zinc batteries, which tend to give a small response. The vapes can also be grouped, though one AA zinc battery is close to a vape measurement.

Fig. 4 (b) shows the reduction of the 168 dimensions to two using PCA when individual scaling is applied. We see a grouping of D and E batteries again, with the D battery, which was an outlier previously, now part of the D group. The AA and AAA are grouped together, though some separate grouping can be seen, where the AAA batteries are grouped between two AA batteries. The left group of the batteries is zinc chloride, and the right is alkaline, lithium, and NiMH. These two groups relate to the different metal cylinder materials that both batteries use. Three zinc batteries are now grouped, with the fourth on its own below the E and D groups. Notably, the zinc batteries are no longer grouped close to the vapes. The vapes have their own grouping, which can be seen where no other batteries are close. The groupings give a good discrimination of the vapes from the batteries.

The variance for PCA component 1 is 75.4% and 18.8% for component 2 when the data is not scaled. The variance of PCA when the data is scaled is 66.7% and 20.7% for PCA components 1 and 2, respectively. The total variance of the data preserved is 87.2% when the measurements are not scaled and 87.4% when the measurements are scaled. If the number of PCA components is increased to 3, the total variance increases by 2.79% when the measurements are not scaled and 6.17% when the measurements are scaled. Future work may find that the increase in total variance could improve classification accuracy.

Fig. 5 (a) shows the reduction of the 168 dimension data into two dimensions using LDA, where the batteries are grouped into size, using the leave one out method when global scaling is applied. The D-sized batteries are clearly grouped, and the E-sized batteries are also grouped together, though one vape is near this group. The AA and AAA are all grouped, so it is difficult to separate them from each other. The Zinc batteries which were grouped together or close to the vapes with PCA are now grouped within the AA and AAA groups. There is a large central cluster of vapes, with vapes 1, 2 and 3 separate from this group. In Fig. 4 (a), it can be observed that vapes 2 and 3 are separate from the main group. As LDA is used with the leave one out method, the LDA model needs to be trained first and then used to transform the unseen measurements. As the vapes have no other similar measurements, the model has not been trained on similar measurements, which leads to the measurement not being part of the main cluster.

Fig. 5 (b) shows the reduction of the 168 dimensions to two using LDA, where the batteries are grouped into size, using the leave one out method when individual scaling is applied.

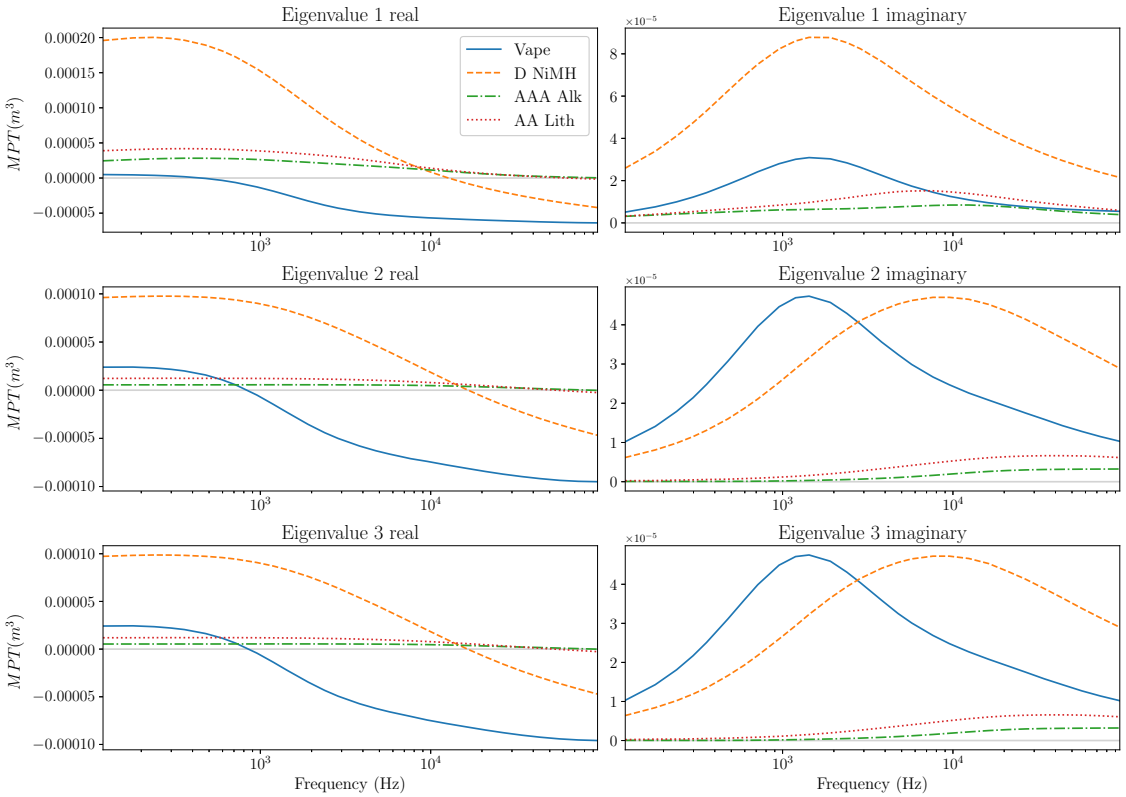

Fig. 3. The complex Eigenvalues of the measured MPTs for one vape and three different battery types. The solid grey line on each plot gives a zero-value reference.

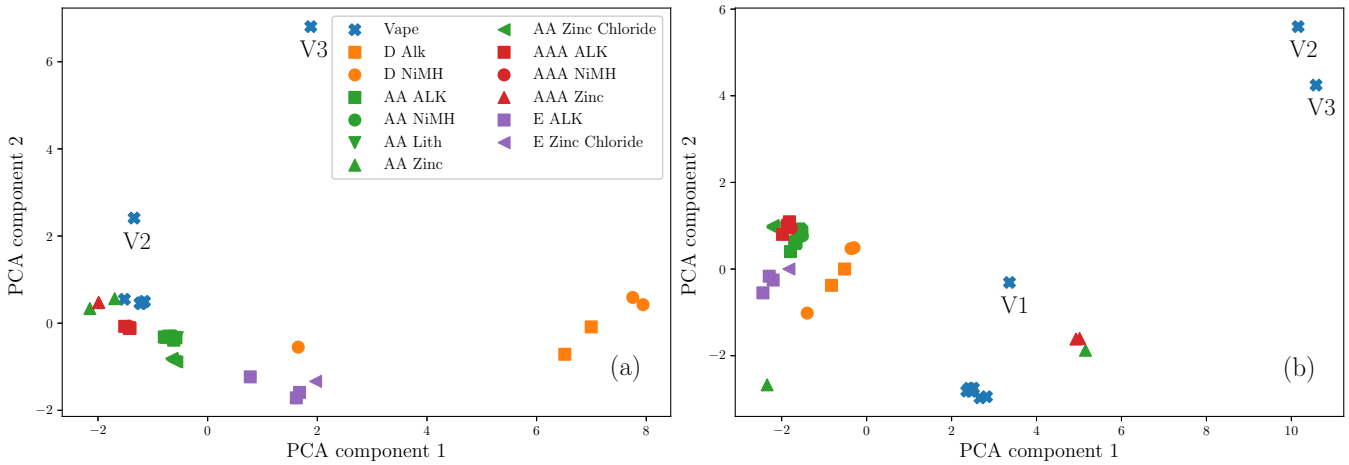

Fig. 4. The PCA transform of 10 vapes and 37 batteries into two components using (a) global measurement scaling and (b) individual measurement scaling prior to applying PCA. Each outlier vape is labelled.

Fig. 5 (b) shows a grouping of all the vapes with no batteries within the group. The batteries are all clustered together and do not have a clear separation into size, as seen in Fig. 4.

Fig. 6 (a) shows the reduction of the 168 dimension data into two dimensions using LDA, where the batteries are grouped into type, using the leave one out method when global scaling is applied. It can be seen in Fig. 6 (a) that there is a cluster of vapes, and as seen previously, vapes 1, 2 and 3 are not near this cluster. Most of the batteries are not clustered, with the only observable clusters being AA zinc chloride and AAA alkaline / NiMH clustered together. Fig. 6 (b) shows the reduction of the 168 dimensions to two using LDA, where the batteries are grouped into size, using the leave one out method when individual scaling is applied. Fig. 6 (b) shows a large grouping of batteries where it is difficult to differentiate them. There is a small grouping of D batteries and E alkaline batteries. The zinc batteries, which were separate from the batteries in Fig. 4 are again separate from the main group of batteries. There is a clear grouping of the vapes away from the batteries, and they are not affected by the separate group of zinc batteries.

The plots in Fig. 6 show that it is difficult to reduce the dimensions with LDA when using the type of battery as a

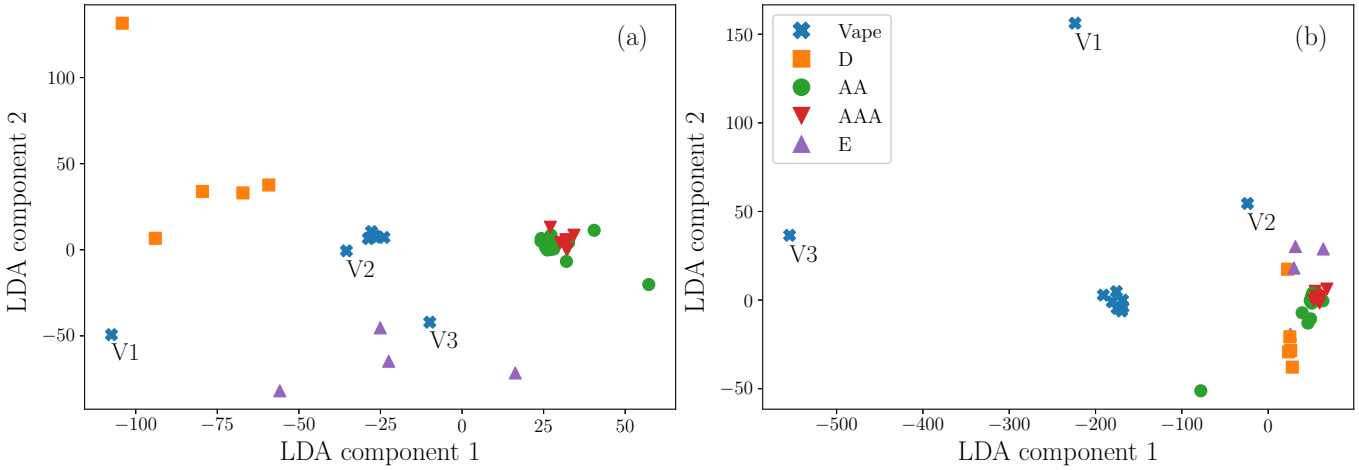

Fig. 5. The LDA transform of 10 vapes and 37 batteries, labelled based on size, into two components using (a) global measurement scaling and (b) individual measurement scaling prior to applying PCA, using leave one out. Each outlier vape is labelled.

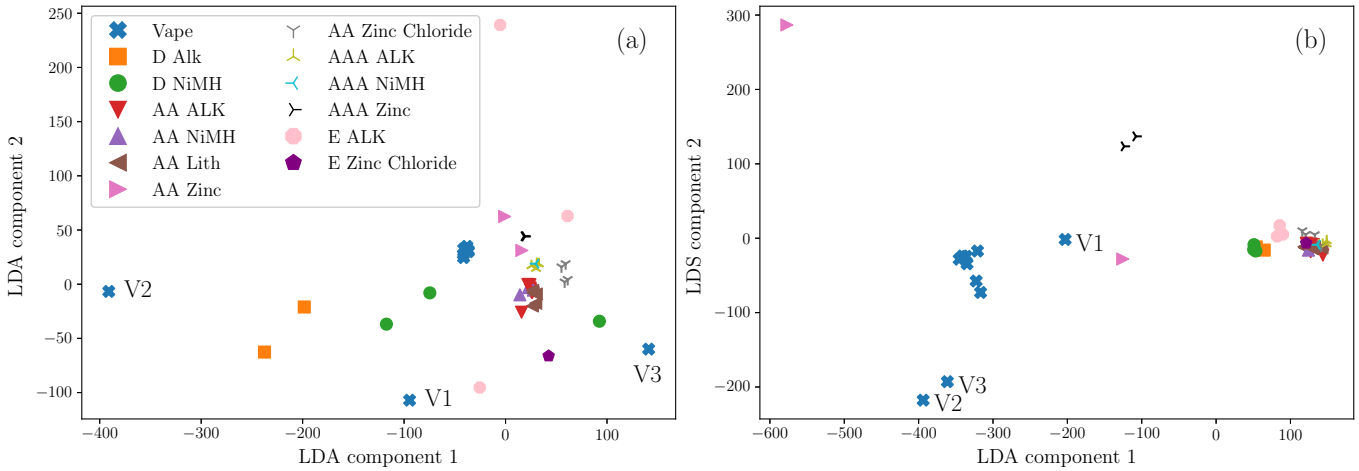

Fig. 6. The LDA transform of 10 vapes and 37 batteries, labelled based on type, into two components using (a) global measurement scaling and (b) individual measurement scaling prior to applying PCA, using leave one out. Each outlier vape is labelled.

label. A cause of this is that the model is being trained to separate measurements where the batteries had similar casing material. The similar casing material will result in similar measurements, which would be difficult to separate. When the batteries were grouped by size in Fig. 4, batteries with similar casing in material and size had the same label, leading to more apparent separation and grouping. A Hitachi VULCAN LIBS analyser was used to acquire the metal composition of the AA batteries' casing and top and bottom contacts. The tested AA alkaline, NiMH, and lithium batteries all have a case and top and bottom contact made from Ni-200, which is a corrosion-resistant nickel alloy. The same casing of the three battery types explains their groupings in the presented results. The zinc chloride battery has a case and top and bottom contacts made from carbon steel (C-steel). Finally, the zinc battery has a bottom contact made from C-steel and a top contact of Ni-200 and the casing is made from a cardboard-like material. The casing material explains the response when the zinc batteries are measured, which is essentially dominated by and approximates the MPT behaviour of a ferromagnetic cylinder.

V. Conclusion

The magnetic polarizability tensor allows for a feature-rich measurement of a metallic object, which, when paired with the dimension reduction techniques PCA and LDA, can create a clear grouping of objects in two dimensions. The magnetic polarizability tensor has been used previously to detect firearms and knives from other objects as they pass through walk-through metal detectors [31]. This article presents the first results of using the magnetic polarizability tensor to classify waste, more specifically, the discrimination of disposable vapes from batteries. The measurements, which consist of 168 features, are reduced to two features to allow for visualisation and dimension reduction. The 168 features consist of the real and imaginary components of the three eigenvalues across 28 frequencies.

When PCA is used, the batteries are grouped into sizes apart from zinc batteries, which are separate from their corresponding size group. The zinc batteries are grouped close to the vapes but are still separable. When the measurements are independently scaled, the grouping of all the batteries and vapes becomes clearer, especially as the vapes and the zinc

batteries have further separation.

When LDA is used, which is trained with the labels of the measurements, the grouping of the vapes and batteries is clear. When the measurements are not independently scaled, there is a grouping of the vapes, though one outlier measurement is close to the E-type batteries. The vape measurement being close to the E-type battery was due to the LDA model not being trained on any measurements similar to outlier measurement. When the measurements are independently scaled, there is a clear differentiation between the vapes and batteries. Though the batteries cannot be separated by size like in PCA, the vapes are separate from the batteries.

Additionally, when LDA was used to separate the vapes from the batteries based on their type, there was no grouping. However, when the measurements were independently scaled, the vapes were grouped away from the batteries. The batteries cannot be easily separated, though some minor groups were present, with the zinc batteries separate from the other batteries. A reason for the poor grouping was that the LDA model was trained on labels based on the battery type and size. The labelling of type and size led to the LDA model trying to separate batteries of similar size and material casing from each other, which would have similar measurements.

The magnetic polarizability tensor has shown to be a useful measurement to use to differentiate vapes from batteries. PCA and LDA have been shown to reduce the dimension of the measurements to two features, which allows visual grouping of the objects. The PCA results are most important as it is not trained with the data labels, so it does not know the label of each measurement. Future work will need to build up a larger measurement library and combine dimension reduction and machine learning techniques to detect vapes in a waste stream for removal. However, more work would be needed to measure and calculate the magnetic polarizability tensor in real time on a moving conveyor belt.

ACKNOWLEDGMENT

The authors would like to thank the UK Engineering and Physical Sciences Research Council (Grant ref EP/W021013/1) for their financial support.

REFERENCES

[1] F. R. M. Ali, A. B. Seidenberg, E. Crane, E. Seaman, M. A. Tynan, K. Marynak, "E-cigarette Unit Sales by Product and Flavor Type, and Top-Selling Brands, United States, 2020–2022," MMWR Morbidity and Mortality Weekly Report, vol. 72, pp. 672–677, 2023.

[2] L. Smith, N. Sutherland, 11The environmental impact of disposable vapes," CDP 2022/0216, London: House of Commons Library, 2022.

[3] A. Mcneill, L. Brose, R. Calder, E. Simonavicius, D. Robson, "Vaping in England: an evidence update including vaping for smoking cessation," a report commissioned by PHE, London: PHE, 2021.

[4] Environment Agency, "Electrical and electronic equipment (EEE) is covered by the WEEE Regulations," 2023. [Online]. Available: https://www.gov.uk/government/publications/electrical-and-electronic-equipment-eee-covered-by-the-weee-regulations/electrical-and-electronic-equipment-eee-covered-by-the-weee-regulations

[5] Material Focus, "Disposable single-use vapes thrown away have quadrupled to 5 million per week," 2023. [Online]. Available: https://www.materialfocus.org.uk/press-releases/disposable-single-use-vapes-thrown-away-have-quadrupled-to-5-million-per-week/

[6] British Geological Survey, "UK criticality assessment of technology critical minerals and metals," 2022. [Online]. Available: https://www.bgs.ac.uk/download/uk-criticality-assessment-of-technology-critical-minerals-and-metals/

[7] Department for Business, Energy and Industrial Strategy, "Resilience for the Future: The UK's Critical Minerals Strategy," 2023. [Online]. Available: https://www.gov.uk/government/publications/uk-critical-mineral-strategy/resilience-for-the-future-the-uks-critical-minerals-strategy

[8] P. Greim, A. A. Solomon, C. Breyer, "Assessment of lithium criticality in the global energy transition and addressing policy gaps in transportation," Nature Communications, vol. 11, pp. 1–11, 2020.

[9] A. Sonoc, J. Jeswiet, "A review of lithium supply and demand and a preliminary investigation of a room temperature method to recycle lithium ion batteries to recover lithium and other materials," Procedia CIRP, vol. 15, pp. 289–293, 2014.

[10] A. M. Bernardes, D. C. R. Espinosa, J. A. S. Tenório, "Recycling of batteries: A review of current processes and technologies," Journal of Power Sources, 130, 291–298, 2004.

[11] A. Sonoc, J. Jeswiet, V. K. Soo, "Opportunities to improve recycling of automotive lithium ion batteries," Procedia CIRP, vol. 29, 2015.

[12] M. Brown, M. Hilton, S. Crossette, M. Hickman, R. Mason, A. Brown, "Cutting lithium-ion battery fires in the waste industry," 2021. [Online]. Available: https://www.eunomia.co.uk/reports-tools/cutting-lithium-ion-battery-fires-in-the-waste-industry/

[13] Material Focus, "Over 700 fires in bin lorries and recycling centres are caused by batteries many of which are hidden inside electricals," 2022. [Online]. Available: https://www.materialfocus.org.uk/press-releases/over-700-fires-in-bin-lorries-and-recycling-centres-are-caused-by-batteries-many-of-which-are-hidden-inside-electricals/

[14] R. F. Mikalsen, A. Lönnermark, K. Glansberg, M. McNamee, K. Storesund, "Fires in waste facilities: Challenges and solutions from a Scandinavian perspective," Fire Safety Journal, vol. 120, 2021.

[15] R. F. Mikalsen, K. Glansberg, K. Storesund, S. Ranneklev, "Branner i avfallsanlegg," 2019. [Online]. Available: https://www.diva-portal.org/smash/record.jsf?pid=diva2%3A1371471&dswid=-4395

[16] K. C. Williams, M. D. O'Toole, L. A. Marsh, A. J. Peyton, "Classification of batteries in waste streams using magnetic induction spectroscopy," in Proc. IEEE Sensors Applications Symposium (SAS), pp. 1-6 2022

[17] F. Gu, J. Guo, X. Yao, P. A. Summers, S. D. Widijatmoko, P. Hall, "An investigation of the current status of recycling spent lithium-ion batteries from consumer electronics in China," Journal of Cleaner Production, vol. 161, pp. 765–780, 2017.

[18] L. Li, J. Lu, Y. Ren, X. X. Zhang, R. J. Chen, F. Wu, K. Amine, "Ascorbic-acid-assisted recovery of cobalt and lithium from spent Li-ion batteries," Journal of Power Sources, vol. 218, pp. 21–27, 2012.

[19] M. B. Mesina, T. P. R. de Jong, W. L. Dalmijn, "New developments on sensors for quality control and automatic sorting of non-ferrous metals," IFAC Proceedings Volumes, vol. 37, pp 293–298, 2004.

[20] M. B. Mesina, T. P. R. de Jong, W. L. Dalmijn, "Improvements in separation of non-ferrous scrap metals using an electromagnetic sensor," Physical Separation in Science and Engineering, vol. 12, 2003.

[21] M. Kutila, J. Viitanen, A. Vattulainen, "Scrap metal sorting with colour vision and inductive sensor array," International Conference on Computational Intelligence for Modelling, Control and Automation, and International Conference on Intelligent Agents, Web Technologies and Internet Commerce, vol. 2, pp. 725–729, 2005.

[22] M. D. O'Toole, N. Karimian, A. J. Peyton, "Classification of nonferrous metals using magnetic induction spectroscopy," IEEE Transactions on Industrial Informatics, vol. 14, pp. 3477–3485, 2018.

[23] M. D. O'Toole, A. J. Peyton, "Classification of Non-ferrous Scrap Metal using Two Component Magnetic Induction Spectroscopy," in Proc. IEEE Sensors Applications Symposium (SAS), 2019.

[24] K. C. Williams, M. D. O'Toole, M. J. Mallaburn, A. J. Peyton, "A review of the classification of non-ferrous metals using magnetic induction for recycling," Insight: Non-Destructive Testing and Condition Monitoring, vol. 65, pp 384–388, 2023.

[25] K. C. Williams, M. D. O'Toole, A. J. Peyton, "Scrap Metal Classification Using Magnetic Induction Spectroscopy and Machine Vision," IEEE Transactions on Instrumentation and Measurement, vol. 72, 2023.

[26] K. C. Williams, M. J. Mallaburn, M. Gagola, M. D. O'Toole, R. Jones, A. J. Peyton, "Classification of Shredded Aluminium Scrap Metal Using Magnetic Induction Spectroscopy," Sensors, vol. 23, 2023.

[27] J. P. Fernández, B. E. Barrowes, T. M. Grzegorczyk, N. Lhomme, K. O'Neill, F. Shubitidze, F, "A man-portable vector sensor for iden-

tification of unexploded ordnance," IEEE Sensors Journal, vol. 11, pp.2542–2555, 2011.
[28] S. J. Norton, I. J. Won, "Identification of buried unexploded ordnance from broadband electromagnetic induction data," IEEE Transactions on Geoscience and Remote Sensing, vol. 39, pp. 2253–2261, 2001.
[29] T. M. Grzegorczyk, B. E. Barrowes, F. Shubitidze, J. P. FernÁndez, K. O'Neill, "Simultaneous identification of multiple unexploded ordnance using electromagnetic induction sensors," IEEE Transactions on Geoscience and Remote Sensing, vol. 49, pp. 2507–2517, 2011.
[30] H. H. Nelson, J. R. McDonald, "Multisensor towed array detection system for UXO detection," IEEE Transactions on Geoscience and Remote Sensing, vol. 39, pp. 1139–1146, 2001.
[31] J. L. Davidson, T. Ozdeger, D. Conniffe, M. Murray-Flutter, A. J. Peyton, "Classification of Threat and Nonthreat Objects Using the Magnetic Polarizability Tensor and a Large-Scale Multicoil Array," IEEE Sensors Journal, vol. 23, pp. 1541–1550, 2023.
[32] T. Õzdeğer, J. L. Davidson, P. D. Ledger, D. Conniffe, W. R. B. Lionheart, A. J. Peyton "Measuring the Magnetic Polarizability Tensor of Nonsymmetrical Metallic Objects," IEEE Sensors Journal, vol. 23, pp. 20027–20036, 2023.
[33] W. R. Scott, G. D. Larson "Modeling the measured EM induction response of targets as a sum of dipole terms each with a discrete relaxation frequency," International Geoscience and Remote Sensing Symposium (IGARSS), pp. 4188–4191, 2010.
[34] G. D. Larson, W. R. Scott, "Automated, non-metallic measurement facility for testing and development of electromagnetic induction sensors for landmine detection," SPIE, 2009.
[35] O. A. Abdel-Rehim, J. L. Davidson, L. A. Marsh, M. D. O'Toole, A. J. Peyton, "Magnetic Polarizability Tensor Spectroscopy for Low Metal Anti-Personnel Mine Surrogates," IEEE Sensors, vol. 16, 2016.
[36] M. Simic, D. Ambrus, V. Bilas, "Inversion-Based Magnetic Polarizability Tensor Measurement From Time-Domain EMI Data," IEEE Transactions on Instrumentation and Measurement, 72, 2023.
[37] J. Kauppila, T. Ala-Kleemola, J. Vihonen, J. Jylhä, M. Ruotsalainen, A, Jarmo Kauppila, A. Järvi, A. Visa, "Classification of items in a walk-through metal detector using time series of eigenvalues of the polarizability tensor," vol. 7303, pp. 185–194, 2009.
[38] J. Makkonen, L. A. Marsh, J. Vihonen, A. Järvi, D. W. Armitage, A. Visa, A. J. Peyton, "KNN classification of metallic targets using the magnetic polarizability tensor," Measurement Science and Technology, vol. 25, 2014.
[39] J. Makkonen, L. A. Marsh, J. Vihonen, A. Järvi, D. W. Armitage, A. Visa, A. J. Peyton, A. J, "Improving reliability for classification of metallic objects using a WTMD portal," Measurement Science and Technology, vol. 26, 2015.
[40] A. R. Al-Qubaa, A. Al-Shiha, G. Y. Tian, "Threat target classification using ANN and SVM based on a new sensor array system," Progress in Electromagnetics Research B, vol. 61, pp. 69–85, 2014.
[41] D. K. Kotter, L. G. Roybal, R. E. Polk, "Detection and classification of concealed weapons using a magnetometer-based portal," SPIE Defense + Commercial Sensing, vol. 4708, pp. 145–155, 2002.
[42] O. A. Abdel-Rehim, J. L. Davidson, L. A. Marsh, M. D. O'Toole, A. J. Peyton, "Magnetic Polarizability Tensor Spectroscopy for Low Metal Anti-Personnel Mine Surrogates," IEEE Sensors, vol. 16, 2016.
[43] B. A. Wilson, P. D. Ledger, W. R. B. Lionheart, "Identification of metallic objects using spectral magnetic polarizability tensor signatures: Object classification," International Journal for Numerical Methods in Engineering, vol. 123, pp. 2076–2111, 2022.
[44] H. Ammari, J. Chen, z. Chen, J. Garnier, D. Volkov, "Target detection and characterization from electromagnetic induction data," Journal de Mathématiques Pures et AppliquÉes., vol. 101, pp 54–75, 2014.
[45] P. D. Ledger, W. R. B. Lionheart, "Characterizing the shape and material properties of hidden targets from magnetic induction data," IMA Journal of Applied Mathematics," vol. 80, pp. 1776–1798, 2015.
[46] P. D. Ledger, W. R. B. Lionheart, "Understanding the Magnetic Polarizability Tensor," IEEE Transactions on Magnetics, voL. 52, 2016.
[47] P. D. Ledger, W. R. B. Lionheart, "The spectral properties of the magnetic polarizability tensor for metallic object characterisation," Mathematical Methods in the Applied Sciences, vol 43, 2020.
[48] P. D. Ledger, W. R. B. Lionheart, "An Explicit Formula for the Magnetic Polarizability Tensor for Object Characterization," IEEE Transactions on Geoscience and Remote Sensing, vol. 56, pp. 3520–3533, 2018.
[49] A. Géron, "Hands-On Machine Learning with Scikit-Learn, Keras, and TensorFlow - Concepts, Tools, and Techniques to Build Intelligent Systems," 2nd ed. O'Reilly Media, 2019
[50] A. Maćkiewicz, W. Ratajczak, "Principal components analysis (PCA)," Computers and Geosciences, vol. 19, pp. 303–342, 1993.
[51] K. Pearson. "On lines and planes of closest fit to systems of points in space. The London, Edinburgh, and Dublin Philosophical Magazine and Journal of Science," vol. 2, pp 559–572, 2010.
[52] T. Õzdeğer, J. L. Davidson, W. van Verre, L. A. Marsh, W. R. B. Lionheart, A. J. Peyton, "Measuring the Magnetic Polarizability Tensor Using an Axial Multi-Coil Geometry," IEEE Sensors Journal, vol. 21, pp. 19322–19333, 2021.
[53] L. A. Marsh, C. Ktistis, A. Järvi, D. W. Armitage, A. J. Peyton, A. J. "Three-dimensional object location and inversion of the magnetic polarizability tensor at a single frequency using a walk-through metal detector," Measurement Science and Technology, vol. 24, 2013.

Kane C. Williams received the B.Eng (Hons.) degree in electronic engineering with industrial experience from The University of Manchester in 2020. He is currently undertaking a PhD at The University of Manchester. His research focuses on classifying and sorting scrap waste using machine learning and different sensors for non-destructive inspection. His research interests include machine learning, embedded systems and computer vision and sensor fusion.

John L. Davidson received a B.Sc. (Hons.) degree in engineering physics and a Ph.D. degree in Mössbauer spectroscopy from Sheffield Hallam University, Sheffield, U.K., in 1993 and 1997, respectively. As a Research Fellow with the University of Southampton, Southampton, U.K., from 1998 to 2002, he developed an interest in electromagnetics. In 2002, he joined The University of Manchester, Manchester, U.K., initially working in the area of electrical impedance tomography applied to industrial and medical problems and, more recently, in the area of electromagnetics. He has authored or co-authored more than 50 scientific publications. His research interests include electromagnetic modelling, inverse problems, and magnetic induction sensor development. Dr. Davidson received the Beloe Fellowship Award from the Worshipful Company of Scientific Instrument Makers in 2008.

Michael D. O'Toole received the M.Eng. (Hons.) degree in integrated engineering from the University of Reading in 2006, and the Ph.D. from the Wolfson School of Mechanical and Manufacturing Engineering, Loughborough University, in 2011. He was a Research Associate at The University of Manchester from 2011 to 2016 working primarily on magnetic induction systems for non-destructive inspection and characterisation. He was awarded a Leverhulme Trust Early Career Research Fellowship in 2016, and appointed lecturer in 2020. He is author and co-author of over 20 scientific publications and has recently filed his first patent. His research interests include signal processing, and sensor and instrumentation design, with a particular emphasis on magnetic induction systems for non-destructive testing.

Anthony J. Peyton received the B.Sc. degree in electrical engineering and electronics and Ph.D. in medical instrumentation from UMIST in 1983 and 1986, respectively. He was appointed Principal Engineer at Kratos Analytical Ltd. in 1989, developing precision electronic instrumentation for magnetic sector and quadrupole mass spectrometers. He returned to UMIST as a Lecturer and worked with the Process Tomography Group. He moved to Lancaster University in 1996 as Senior Lecturer, was promoted to Reader in electronic instrumentation in 2001 and Professor in 2004. Since 2004, he has been a Professor of Electromagnetic Tomography Engineering at the University of Manchester. He has been a Principal Investigator of numerous national and industry funded projects and a partner of ten previous EU projects. He is a co-author on over 110 international journal papers, two books, several hundred conference papers, and 12 patents in areas related to electromagnetics and tomography.